Lateral-Directional Stability and Control Characteristics of the Quiet Short-Haul Research Aircraft (QSRA)

Jack D. Stephenson, James A. Jeske, and Gordon H. Hardy, Ames Research Center, Moffett Field, California

May 1990

NASA

National Aeronautics and
Space Administration

Ames Research Center
Moffett Field, California 94035-1000

NOMENCLATURE

a_Y	lateral acceleration, g
b	wing span, ft
C_{D_R}	ram drag coefficient
C_l	rolling moment coefficient
C_L	lift coefficient
C_n	yawing moment coefficient
C_T	thrust coefficient
C_Y	side force coefficient
C_μ	aileron BLC momentum coefficient (written as Cmu_AIL in table 3)
g	acceleration of gravity
I_X, I_Y, I_Z	moment of inertia about the X-, Y-, and Z-axis, slug-ft^2
I_{XZ}	product of inertia, slug-ft^2
m	aircraft mass, slugs
$\dot{m}_J$	aileron BLC nozzle mass flow rate, slugs/sec
$\dot{M}$	engine air mass flow rate, slugs/sec
p, q, r	roll, pitch and yaw rates, deg/sec or rad/sec
$\overline{q}$	dynamic pressure, lb/sq ft
S	wing area
T	engine thrust, lb
V	true airspeed, ft/sec
V_J	aileron BLC nozzle flow velocity, ft/sec
W	gross weight, lb
S_{WA}	reference area for defining C_μ, sq ft
X_I, Z_I	longitudinal and vertical distances from the engine inlets to the c.g., ft
α	angle of attack, deg
β	sideslip angle, deg or rad
δ_A	aileron deflection, deg or rad
δ_R	rudder deflection, deg or rad
δ_S	spoiler deflection, deg or rad
δ_W	wheel deflection, deg
ϕ	roll angle, deg
$(\dot{\ })$	derivative with respect to time

Subscripts

o	initial condition
e	based on estimates

Abbreviations

BLC	boundary layer control
DLC	direct lift control
USB	upper surface blown (flaps)

Symbols identifying the stability and control derivatives in the figures are defined as follows:

$$C_{l_\beta} = \frac{\partial C_l}{\partial \beta} \qquad\qquad C_{n_\beta} = \frac{\partial C_n}{\partial \beta} \qquad\qquad C_{Y_\beta} = \frac{\partial C_Y}{\partial \beta}$$

$$C_{l_p} = \frac{\partial C_l}{\partial(\frac{pb}{2V})} \qquad\qquad C_{n_p} = \frac{\partial C_n}{\partial(\frac{pb}{2V})} \qquad\qquad C_{Y_p} = \frac{\partial C_Y}{\partial(\frac{pb}{2V})}$$

$$C_{l_{RUD}} = \frac{\partial C_l}{\partial \delta_R} \qquad\qquad C_{n_{RUD}} = \frac{\partial C_n}{\partial \delta_R} \qquad\qquad C_{Y_{RUD}} = \frac{\partial C_Y}{\partial \delta_R}$$

$$C_{l_{\delta_A}} = \frac{\partial C_l}{\partial \delta_A} \qquad\qquad C_{n_{\delta_A}} = \frac{\partial C_n}{\partial \delta_A} \qquad\qquad C_{Y_{\delta_A}} = \frac{\partial C_Y}{\partial \delta_A}$$

$$C_{l_{\delta_S}} = \frac{\partial C_l}{\partial \delta_S} \qquad\qquad C_{n_{\delta_S}} = \frac{\partial C_n}{\partial \delta_S} \qquad\qquad C_{Y_{\delta_S}} = \frac{\partial C_Y}{\partial \delta_S}$$

$$C_{l_r} = \frac{\partial C_l}{\partial(\frac{rb}{2V})} + \frac{\partial C_l}{\partial(\frac{\dot\beta b}{2V})}$$

$$C_{n_r} = \frac{\partial C_n}{\partial(\frac{rb}{2V})} + \frac{\partial C_n}{\partial(\frac{\dot\beta b}{2V})}$$

$$C_{Y_r} = \frac{\partial C_Y}{\partial(\frac{rb}{2V})} + \frac{\partial C_Y}{\partial(\frac{\dot\beta b}{2V})}$$

$$C_{l_{LAT}} = \frac{\partial C_l}{\partial \delta_A} + \frac{\partial C_l}{\partial \delta_S} \qquad\qquad C_{n_{LAT}} = \frac{\partial C_n}{\partial \delta_A} + \frac{\partial C_n}{\partial \delta_S}$$

$$C_{l_\delta} = \frac{\partial C_l}{\partial \delta_S} \qquad\qquad C_{n_\delta} = \frac{\partial C_n}{\partial \delta_S}$$

The column headings in tables 2, 3, and 4 refer to the stability derivatives listed above as follows:

CLB = C_{l_β}	CNB = C_{n_β}	CYB = C_{Y_β}
CLP = C_{l_p}	CNP = C_{n_p}	CYP = C_{Y_p}
CLR = C_{l_r}	CNR = C_{n_r}	CYR = C_{Y_r}
CLRUD = $C_{l_{RUD}}$	CNRUD = $C_{n_{RUD}}$	CYRUD = $C_{Y_{RUD}}$
CLAIL = $C_{l_{\delta_A}}$	CNAIL = $C_{n_{\delta_A}}$	CYAIL = $C_{Y_{\delta_A}}$
CLSP = $C_{l_{\delta_S}}$	CNSP = $C_{n_{\delta_S}}$	CYSP = $C_{Y_{\delta_S}}$
CLLAT = $C_{l_{LAT}}$	CNLAT = $C_{n_{LAT}}$	
CLSD = C_{l_δ}	CNSD = C_{n_δ}	

The last two of these derivatives are in units of $(rad/sec)^{-1}$. All of the other derivatives are given in $(rad)^{-1}$.

SUMMARY

This report presents the results of flight experiments to determine the lateral-directional stability and control characteristics of the Quiet Short-Haul Research Aircraft (QSRA), an experimental aircraft designed to furnish information on various aerodynamic characteristics of a transport type of airplane that makes use of the upper-surface blown (USB) flap technology to achieve short takeoff and landing (STOL) performance. The flight program designed to acquire the data consisted of maneuvers produced by rudder and control-wheel inputs with the airplane in several configurations that had been proposed for landing approach and takeoff operation. The normal stability augmentation system was not engaged during these maneuvers. Time-history records from the maneuvers were analyzed with a parameter estimation procedure to extract lateral-directional stability and control derivatives. For one aircraft configuration in which the USB flaps were deflected $50°$, several maneuvers were performed to determine the effects of varying the average angle of attack, varying the thrust coefficient, and setting the airplane's upper surface spoilers at a $13°$ symmetrical bias angle. The effects on the lateral characteristics of deflecting the spoilers were rather small and generally favorable. The data indicate that for one test, conducted at low thrust (a thrust coefficient of 0.38), compared with results from tests at thrust coefficients of 0.77 and larger, there was a significant decrease in the lateral control effectiveness, in the yaw damping and in the directional derivative (C_{n_β}). The directional derivative was also decreased (by about 30%) when the average angle of attack of the test was increased from $3°$ to $16°$.

INTRODUCTION

The Quiet Short-Haul Research Aircraft (QSRA) was designed and built to provide flight experience in a program to study the characteristics of an airplane employing the upper-surface blown (USB) powered-lift concept. Flight experiments were conducted to acquire data that could be analyzed to provide longitudinal and lateral-directional static and dynamic stability derivatives for the airplane without stability augmentation. Results of these tests to determine the longitudinal stability characeristics have been reported in reference 1. Results of the tests to study the lateral-directional characteristics are presented in this report. The tests covered a range of engine thrust levels and airspeeds, in several configurations that had been considered suitable for landing approach and one configuration considered optimum for takeoff. Time history records of the airplane's response to rudder and control-wheel inputs were analyzed with a linear-regression parameter estimation procedure to extract estimates of the lateral-directional stability and control derivatives.

THE RESEARCH AIRCRAFT

A three-view sketch of the QSRA, with dimensions and areas of various components, is shown in figure 1. Figure 2 is a photograph of the aircraft with the flaps and ailerons deflected to represent a landing approach configuration. References 2 and 3 provide illustrations and other information on the control surfaces whose aerodynamic characteristics were investigated as part of the flight program described herein. The wing of the aircraft was constructed with the USB flaps extending spanwise from the fuselage to 47% semispan. The ailerons, which have upper-surface boundary-layer-control blowing, extend from a spanwise station at 70% semispan outward to the wing tip. The pilot's control wheel drives a dual hydraulic

tandem actuator to operate the ailerons. Between the ailerons and the USB flaps, the wing is fitted with conventional double-slotted trailing-edge flaps.

Upper surface spoilers consisting of two surfaces, an outboard and an inboard section, on each wing panel are located ahead of the slotted flaps. They are operated differentially by control-wheel deflection through hydraulic actuators to provide roll control, augmenting that of the ailerons. Figure 3 shows a static calibration of the deflection angles of the ailerons and the spoilers as functions of the control wheel angle. Also, all of the spoilers can be deflected together (symmetrically) to provide direct lift control (DLC) in addition to their function as a lateral control. The rudder on the airplane is double-hinged, with the rear portion deflecting up to 50° (measured from the aircraft centerline), twice that of the forward section. The airplane was fitted with a nose boom on which were mounted an angle-of-attack vane, a sideslip vane, and pitot-static instrumentation. Instrumentation for acquisition of test data provided for onboard recording and telemetry with ground-based recording of more than 100 variables at rates of 100 Hz. Before processing the data, however, the frame rate was reduced by decimation to 20 Hz, and the analysis of the data is based on this rate.

FLIGHT EXPERIMENTS

To obtain the data for this report, the pilots set the requested airplane configuration, thrust level, and airspeed and then executed maneuvers produced by rudder and control wheel inputs. For most of the tests, the motion was excited first by a rudder doublet and then, after a brief time interval, by one or two large amplitude positive and negative wheel excursions. An example of a time-history record from a typical maneuver is shown in figure 4. A few of the maneuvers were responses to wheel inputs only. For all maneuvers, the normal lateral and directional stability augmentation system was turned off. Also for all of the maneuvers, the slotted flaps were set at 59° with an aileron droop angle of 23°. The majority of the tests were performed with the USB flaps at 50° and with the DLC spoilers undeflected. For two of the tests with this USB flap angle, the DLC spoilers were set at a bias angle (of approximately 13°) and kept at this angle, varying only with the aileron deflection as a lateral control. In addition to these tests, two were conducted with the USB flaps undeflected, representing a takeoff configuration; two tests were conducted with 31° USB flap deflection; and one was done with 66° deflection. The maneuvers were done at constant thrust and, to the extent that was practicable, at constant angle of attack, as indicated by a cockpit display of the α vane angle. Strip chart plotting of telemetry data during the tests allowed ground monitoring of some of the variables.

DATA REDUCTION AND ANALYSIS

In the appendix, the equations used to correct the air data measurements are presented. Angle of attack vane measurements were corrected for induced flow angles with equation (7), which was determined empirically from measurements of pitch attitude and flight path angle. Equations (8) and (9) were used to calculate, respectively, the dynamic and the static pressures corrected for position error. A correction to the sideslip vane angle measurement was determined by using the calculation described in the Appendix from reference 4, in which rates of change of side velocity computed using the equations of motion are compared with rates of change of side velocity calculated from the vane measurements. This correction consisted of applying a factor that reduced the measured sideslip angle by 6.5%, for all of the test conditions.

2

Other quantities pertinent to the processing of the data, thrust coefficient C_T, ram drag coefficient C_{D_R} and the momentum coefficient for the aileron boundary-layer-control flow C_μ, were calculated using equations (10) through (13) in the appendix. The data records were smoothed and filtered with the preprocessing program as described by R. E. Bach, Jr. in "State Estimation Applications in Flight-Data Analysis (A User's Manual for SMACK)" (NASA RP, to be published) (where it is included as an initial step of a state estimation analysis). Also, as part of this preprocessing program, angular accelerations needed in the equations of motion were calculated, as the time derivatives of the pitch, roll, and yaw rates. To obtain the lateral-directional stability and control derivatives, the linear-regression parameter estimation procedure described in reference 5 was applied to the smoothed data records, with the following equations assumed to represent the aircraft motion.

Equations of Motion

The following equations of motion used in the analysis of the data are expressed with reference to the airplane body axes. It is assumed that the airplane is a rigid body and that the pitch rates are small.

$$\frac{mg}{\bar{q}S} a_Y = C_Y - C_{D_R} \sin \beta \tag{1}$$

$$\frac{I_X}{\bar{q}Sb}[\dot{p} - \frac{I_{XZ}}{I_X}\dot{r}] = C_l - C_{D_R}\frac{Z_I}{b} \sin \beta \tag{2}$$

$$\frac{I_Z}{\bar{q}Sb}[\dot{r} - \frac{I_{XZ}}{I_Z}\dot{p}] = C_n - C_{D_R}\frac{X_I}{b} \sin \beta \tag{3}$$

where X_I and Z_I are, respectively, the averages of the X- and Z-distances from the engine inlets to the c.g. The moments of inertia, I_X and I_Z, and the product of inertia, I_{XZ}, are plotted as functions of the aircraft gross weight in figure 5. The coefficients C_Y, C_l, and C_n are assumed to be given by the expressions

$$C_Y = C_{Y_o} + \sum_{i=1}^{4} \frac{\partial C_Y}{\partial \xi_i} \xi_i + \sum_{j=1}^{4} \frac{\partial C_Y}{\partial \delta_j} \delta_j \tag{4}$$

$$C_l = C_{l_o} + \sum_{i=1}^{4} \frac{\partial C_l}{\partial \xi_i} \xi_i + \sum_{j=1}^{4} \frac{\partial C_l}{\partial \delta_j} \delta_j \tag{5}$$

$$C_n = C_{n_o} + \sum_{i=1}^{4} \frac{\partial C_n}{\partial \xi_i} \xi_i + \sum_{j=1}^{4} \frac{\partial C_n}{\partial \delta_j} \delta_j \tag{6}$$

The state and input variables, ξ_i and δ_j, are defined as follows.

$$\xi_1 = \beta - \beta_o \qquad \xi_2 = \frac{pb}{2V}$$

$$\xi_3 = \frac{rb}{2V} \qquad \xi_4 = \frac{\dot{\beta}b}{2V}$$

$$\delta_1 = \delta_R - \delta_{R_o} \qquad \delta_2 = \delta_A - \delta_{A_o}$$

$$\delta_3 = \delta_S - \delta_{S_o} \qquad \delta_4 = \dot{\delta}_S$$

3

RESULTS

The aircraft configurations and flight conditions for the tests that provided data presented in this report are listed in table 1. In the first column, each letter, A through E, identifies an airplane configuration, as determined by the deflection angles of the USB flaps and by the symmetrical deflection of the DLC spoilers. Tests A1 through A7 were done with the USB flaps at (nominally) 50° and with the spoilers undeflected. Tests B1 and B2 were done with the same flap angle but with the spoilers deflected as DLC devices 12.1° and 13.2°, respectively. Tests C1 and C2 are with the USB flaps at zero deflection, D1 and D2 are with these flaps at 31°, and E1 is for a 66° deflection. The second and third columns in table 1 indicate the flight number and the order in which the maneuver was performed during the flight. Table 1 also lists the thrust coefficient, lift coefficient, equivalent airspeed, and altitude at the beginning of each maneuver and the average angle of attack and gross weight during the maneuver. The rolling moment, yawing moment, and side force derivatives with respect to sideslip, roll rate, and yaw rate, from the parameter estimation calculations, are shown in table 2.

Table 3 presents the derivatives with respect to rudder angle, aileron angle, and differential spoiler angle. Rudder deflections are measured on the forward section of the double-hinged surface. For one test, C1, the rudder-effect derivatives are omitted because the deflection angles in the data record were in error. In three of the tests (A1, A2, and D2) the rudder was not an input. The rudder derivatives for these tests are shown in parentheses and were entered as fixed not estimated values. Also, fixed values were entered for the derivatives representing the effects of the spoilers (employed as lateral control surfaces). The time-history variations of the spoilers differed enough from those of the ailerons that by including these controls separately, a better fit of the measured and computed accelerations could be obtained. The differences were not large enough, however, to estimate both sets of derivatives. The differences are due to different nonlinearities in the variation of these surfaces with the control wheel deflection and to different lags in their hydraulic actuator systems. In table 3 the column labelled Cmu-AIL is the momentum coefficient of the aileron boundary-layer control flow C_μ.

Some differences in the effects of the lateral control in different maneuvers were observed to be associated with the magnitude of the control deflection employed to excite the maneuver. The maximum angle of deflection of the control surfaces influenced the relation between the aileron and the spoiler deflection. Table 4 shows the maximum deflection angles that the spoilers reached when the control wheel input was applied. Also in table 4 is a column with the heading CNLAT. This is the sum of $\frac{\partial C_n}{\partial \delta_A}$ and $\frac{\partial C_n}{\partial \delta_S}$, an approximate measure of the variation of yawing moment with the deflection of the two control surfaces, the ailerons and spoilers.

When the ailerons and spoilers are deflected for lateral control, the resulting change in lift distribution of the wing produces changes in flow angles at the tail. These changes together with the effect of a lag between the time of the surface deflection and the time for the changes of the flow direction to reach the tail are accounted for in the equations of motion by including the term with $\dot{\delta}_S$ (the rate of deflection of the spoiler) as a variable. Table 4 shows the estimates of the yawing moment and rolling moment derivatives with respect to this variable.

The variation with time of the rolling-moment coefficient, the yawing-moment coefficient, and the side-force coefficient were calculated from the data measurements for each maneuver. Plots of these variations were compared with plots of the variations of these coefficients calculated using the values of the derivatives from the parameter estimation solutions. An example of this comparison is presented in figure 6. For all of the maneuvers listed in the tables, the time histories based on the measurements and on the estimates were in good agreement.

DISCUSSION

Lateral-Directional Stability Derivatives

In figures 7, 8, and 9 the estimated values for the lateral-directional derivatives listed in table 2 are plotted as functions of angle of attack. In these plots the angles of attack are the averages during the maneuvers. Most of the maneuvers were performed with relatively little variation from these averages. In figure 7 the symbols correspond to initial thrust coefficients, which are approximately equal to the thrust coefficients during the time of the maneuvers, because the engine rpm was not varied and the airspeed was maintained approximately constant by the pilot. In figures 8 and 9, the symbols represent data from tests performed with different USB flap angles.

Reference 6 presents a summary of methods based on simplified aerodynamic theory for predicting lateral-directional stability derivatives. Results from this theory indicate that the contributions of the wing to the values of some of the derivatives are functions of the wing lift coefficient. Because the lift coefficient of the QSRA is closely related to C_T, (shown, for example, in ref. 1) the theory would indicate an effect on these derivatives of varying C_T, if the contribution of the wing is important. Most of the results shown in figure 7 are from tests at values of C_T from 0.8 to 1.1. With an increase in C_T to 1.74, (at $\alpha = 2.3°$) the data indicate a small increase in the yaw damping but little change in the other derivatives. A decrease in C_T from 0.8 to 0.38 had a significant effect, decreasing the magnitude of the yaw damping derivative C_{n_r} by about half and C_{n_β} by about 30%. The magnitudes of C_{Y_r} and C_{Y_β} were also decreased by approximately 50% and 30%, respectively, with this decrease in C_T. An effect of varying the angle of attack is noticeable in the derivative C_{n_β} where the increase in α from 3° to 16° decreased this derivative by about 30%. A similar effect on C_{n_β} of increasing α is shown in the data from the tests reported in reference 4. The aircraft that was the subject of the study described in reference 4 had tail components and a fuselage that were essentially the same as those of the QSRA, but a different wing design and engine installation.

In figure 7, two maneuvers are identified with flagged symbols. These are tests B1 and B2 in the tables, maneuvers performed with the DLC spoilers deflected approximately 13° and with the USB flaps at 50°. The graph showing C_{l_β} indicates that deflecting the spoilers increased the dihedral effect by at least 20%. The plots of C_{n_r} indicate that the spoiler deflection increased the yaw damping at the smaller thrust coefficient (1.13) but caused little change at the larger C_T (1.74). In general, deflecting the spoilers did not have significant effects on the values of the other stability derivatives.

Figures 8 and 9 present plots of four of the stability derivatives (C_{l_β}, C_{n_β}, C_{l_p}, and C_{n_r}), obtained from tests with USB flaps set at angles of 0°, 31°, and 66°, compared with the values for the 50° deflection. For two of these flap settings, 0° and 31°, data were available that allow a comparison with data for the 50° flap angle at approximately the same thrust coefficients. No test results were available for the 50° deflection

at the high thrust coefficient (i.e., 2.6) represented by the conditions of the test with the USB flaps at 66°. Results from the latter test are compared with data from test A5, for which the thrust coefficient is 1.74, the largest value of C_T at which data were obtained for the 50° configuration. In figures 8 and 9, the data show little effect of changing the flap angle from 50° to 31°, but a decrease from 50° to 0° decreased C_{n_p} by about 30% and resulted in a small decrease in the magnitude of C_{n_r}. Figure 9 shows that the roll damping derivative C_{l_p} calculated from the test with the USB flaps at 66° was greater in magnitude than that with the 50° deflection, but as mentioned above there was a difference in thrust coeffients that may be the reason for some of this increase.

In figure 10 estimates given in table 2 for the derivatives C_{l_r} and C_{n_p} are plotted for the aircraft with the different USB flap deflection angles. They are shown as functions of the lift coefficient computed for conditions at the start of the maneuver. As in figures 8 and 9, values for the derivatives from data obtained with flap deflections of 0°, 31°, and 66° are compared with the values from tests with the flaps deflected 50°. The figure indicates that the change in C_{l_r} from its value for the 50° deflection to that for any of the other deflection angles was small when compared at similar values of C_L. The magnitude of the estimate for the derivative C_{n_p} at a lift coefficient of 5 for the configuration with the flaps at 31° was more than twice that for the 50° configuration. Results from tests at other conditions, however, indicate that estimates for this derivative are relatively independent of the flap deflection angles, if compared at the same lift coefficient.

Rudder and Lateral Control Effectiveness

Estimates of the derivative $\frac{\partial C_n}{\partial \delta_R}$, the variation of yawing moment coefficient with rudder deflection, are listed in table 3 under the heading CNRUD. Most of the values estimated for this parameter are within the range from 0.35 to 0.41. The differing values do not show a correlation with variations in the test conditions or the airplane configuration. As indicated in reference 2, one of the design goals that had been specified for the aircraft was that the directional control could produce an initial acceleration in yaw of 0.23 radians per second squared under conditions for a normal STOL approach. If it is assumed that the rudder effectiveness is a linear function in the range of rudder deflection to its maximum of 25° and is represented by the values for $\frac{\partial C_n}{\partial \delta_R}$ listed in table 3, calculations indicate that this goal would be exceeded in STOL approaches and under the other conditions of the test maneuvers at airspeeds at least as low as 70 knots.

The effectiveness of the lateral control system of the QSRA in a configuration for STOL approach was investigated as part of the flight program reported in reference 7. Results presented in this reference indicate that the initial roll acceleration produced by full deflection of the control wheel (for the design airspeed and aircraft gross weight) met the design goal for this acceleration, 0.8 radians per second squared. Results of tests to determine effectiveness of this control for the aircraft with other USB flap deflections and at other test conditions are given in the present report. Deflection angles of the ailerons and the spoilers as functions of the control-wheel angle were measured with the airplane on the ground under conditions for which there would be no aerodynamic loads and no effect of a time lag in the system. This is the static calibration shown in figure 3. The relationship of the spoiler deflection to the aileron deflection shown in this plot is representative of that existing during the test maneuvers for which the maximum angles of deflection of the control wheel were relatively limited, i. e., the maximum spoiler angles were less than about 35°. Table 4, in which the maximum spoiler angles are listed, shows that tests A4, A6,

6

A7, B2, D1, and D2 were performed with these limited-angle inputs. For the other tests, the control-wheel excursions were large and, as shown in table 4, the spoilers deflected more than 55°. Records of the surface deflection time histories from these tests show that the relationship of the spoiler and aileron deflections were significantly different from that illustrated in figure 3. The differences depended upon the rates at which the surfaces were moved and the length of time the control surface was held at the large angles. Figure 11 illustrates examples of time histories of the aileron and spoiler deflections from two maneuvers, one (test A6) in which the maximum deflections were limited and one (test A1) that had large positive and negative deflections.

In the equations of motion presented earlier, the effects of the lateral control are expressed as forces and moments proportional to the aileron deflection plus those proportional to the spoiler deflection. Because the parameter estimation computations would not produce reliable values within a single solution for both the aileron and the spoiler derivatives, the calculations were executed with fixed values for one or the other of these derivatives. Values listed in the tables are taken from solutions in which the derivatives defined with respect to the spoiler deflection were fixed. The values that were chosen (shown in parentheses) undoubtedly are inaccurate by varying amounts, but their use allows the calculations to include some of the effects of the varying relationships of the aileron and spoiler deflections. When the lateral control inputs were represented in the equations of motion by the two separate terms, the computed acceleration time-histories consistently displayed better fits to the measurements than when represented by a single term (such as one based only on the control-wheel or aileron deflection). Table 3 lists the values extracted from the data for the aileron derivatives and the values set to represent the spoiler derivatives. One parameter that has been shown in wind tunnel tests to have an important influence on the performance of the lateral control is the strength of the blowing for aileron boundary-layer control. A measure of this parameter, the momentum coefficient C_μ for this blowing, is listed in table 3 as Cmu-AIL.

Any quantitative description of the effects of the variables on the lateral control effectiveness requires a means of combining the derivatives that apply to the two lateral control surfaces. Because of the varying relationship of the spoiler deflection to the aileron deflection, mentioned above, there is no unambiguous rule for combining them. However, for the purpose of discussing the effects of varying the test conditions, it is useful to choose simply the sum of the two derivatives (aileron and spoiler) as an effective lateral control derivative. The quantities $C_{l_{LAT}}$, $C_{n_{LAT}}$, and $C_{Y_{LAT}}$ are defined in this way to represent approximately the rolling moment, yawing moment, and side force due to lateral control deflection. These quantities are plotted in figure 12 for the aircraft configuration with the USB flaps deflected 50°. The yawing moment parameters based on this definition are listed (as CNLAT) in table 4.

For the configuration with the USB flaps at 50°, figure 12 shows that there was a decrease by more than 15% in the rolling effectiveness parameter $C_{l_{LAT}}$ when the thrust coefficient was decreased from 0.85 to 0.38 and C_μ decreased from 0.095 to 0.044. At thrust coefficients in the range from 0.8 to 0.9, data were obtained for this configuration that show some effect of angle of attack variation. An increase in α from 3° to 16° decreased this roll effectiveness by about 20%. Data from tests B1 and B2 indicate that setting the spoilers at an angle of deflection (of 13°) increased the effectiveness by a small amount. The lateral control was slightly less effective with the USB flaps undeflected than with 50° deflection. Table 3 shows that a value for $C_{l_{LAT}}$ calculated for the test in which the USB flaps were deflected 66° would be 0.55 (0.40 plus 0.15), which is significantly larger than the values from the other tests. This large value is partly attributable to the large value of the thrust coefficient (2.57). Estimated values for $C_{n_{LAT}}$ listed in table 4 (and plotted in figure 12 for the configuration with the USB flaps at 50°) indicate that the yawing moment

7

resulting from the lateral control deflection was favorable for all of the test maneuvers. The control inputs that included large spoiler deflections generally resulted in the most favorable (positive) values for $C_{n_{LAT}}$.

The terms assumed to represent the input functions in the equations of motion, equations 1 through 6, include terms assumed to be proportional to the rate of deflection of the spoilers, in addition to those proportional to the deflections of the spoilers, ailerons, and rudder. They are included to account for any effect of a lag in the changes in flow direction in the region of the tail, changes induced by changes in the wing lift distribution, when the lateral control surfaces are deflected. The yawing- and rolling-moment derivatives associated with these terms, $C_{n_{\dot{s}}}$ and $C_{l_{\dot{s}}}$, respectively, are listed in table 4 under the headings CNSD and CLSD. The values for the aircraft with the USB flaps at 50° are plotted in figure 13. This figure and table 4 show that for all of the tests in which the maximum spoiler angles were more than 10°, the estimated values for $C_{n_{\dot{s}}}$ are negative. This indicates that part of the favorable yawing moment due to the lateral control is a result of an induced sidewash. When this control is moved rapidly, the favorable yawing moment response is preceded by a transient that for a brief interval reduces this moment. The rolling moment derivatives $C_{l_{\dot{s}}}$ are also all negative. This indicates that, because $C_{l_{LAT}}$ includes the induced flow effects, the immediate roll response to rapid movements of the control surfaces is slightly less than that indicated by the values of $C_{l_{LAT}}$ in figure 12. These induced flow effects are qualitatively similar to those that were observed in the data from tests of the augmented jet-flap aircraft reported in reference 4.

CONCLUDING REMARKS

Experiments have been conducted to determine lateral-directional stability characteristics of the QSRA, an experimental airplane designed to provide information on various flight characteristics of an aircraft that employs the upper surface blown (USB) flap powered-lift technology. Data records from maneuvers produced by control-wheel and rudder inputs were analyzed with a parameter estimation procedure to extract stability and control derivatives for the airplane in several configurations and at various angles of attack and levels of engine thrust. The maneuvers were conducted with the normal stability augmentation system of the aircraft turned off. The USB flaps, which are mounted on the wing behind the engines and extend spanwise from the fuselage outward to the 47% semispan station, augment the wing lift by causing a deflection of the engine exhaust and increasing the circulation. Other features of the airplane's design include trailing-edge slotted flaps extending out to the 70% semispan station and, outboard of these, ailerons with bounday-layer control. All of the tests described in this report were conducted with the slotted flaps deflected approximately 59° and with the ailerons drooped 23°. Most of the test maneuvers were performed with the USB flaps set (nominally) at 50°. In addition to these, a limited number of tests were also conducted with these flaps at 0°, 31°, and 66°.

Results were obtained with the USB flaps at 50° that provided information on the effects of varying the thrust coefficient (C_T) and angle of attack (α), and of symmetrically deflecting upper-surface spoilers. A decrease in C_T from 0.8 to 0.38 decreased the yaw damping by about 50% and decreased the derivative C_{n_β} by about 30%. An increase in α from 3° to 16° caused a decrease of about 30% in the value of C_{n_β}. The data indicate that a 13° symmetrical deflection of the spoilers resulted in a small increase in the dihedral effect and slightly more yaw damping. The effects on most of the stability derivatives of setting the different USB flap angles were generally small, but the data indicate that when this flap angle was changed from 50° to zero, there was a decrease of about 30% in the value of C_{n_β}.

From earlier tests, it had been determined that the rudder and the lateral control were effective in providing yawing and rolling accelerations that met or exceeded the levels that had been specified as goals for the airplane's design conditions. The tests described in this report indicate that these controls were effective for the various configurations and throughout the ranges of angle of attack (up to 18°) that were investigated. The effectiveness of the lateral control was somewhat reduced when the test was conducted at a reduced thrust level, corresponding to a value of C_T of 0.38, compared with other tests for which C_T was 0.77 and larger. The variation of yawing moment coefficient with lateral control deflection was positive in sign for all of the test conditions. Results based on determination of the yawing moment associated with the rate of deflection of the lateral control surfaces indicate that there is an induced sidewash that provides some of the favorable variation of yawing moment with control deflection.

APPENDIX

DATA REDUCTION FORMULAS

Corrections to aerodynamic data that were applied as part of the data reduction are from tests conducted prior to those that are the subject of this report. The vane-indicated angle of attack, α_i, was corrected by adding the increment $\Delta \alpha$, given by the following formula, in degrees.

$$\Delta \alpha = -1.5[1. + 0.0182(\delta_u - 55.)] - 0.12[1. + 1.5(\delta_u - 55.) + 0.0108(N - 60.)]\alpha_i$$
$$- 0.0021\alpha_i^2 \tag{7}$$

where δ_u is the USB flap deflection angle in degrees and N is the engine fan percent rpm, averaged among the engines. The sideslip angle β for all test conditions was computed as 93.5% of the angle indicated by the sideslip angle vane. This correction to the measurement was determined by the method described in reference 4. In this method the correction factor is determined by matching the rate of change of the side velocity computed from the vane measurement with this change computed from the side acceleration, roll and yaw rates, velocity, and attitude time histories.

Pitot static data corrections had been determined from low level flights in calm air under conditions where the true speed could be measured and the air density was known. The following formula was used to compute a correction which was added to the indicated airspeed (V_i, knots).

$$\Delta V = 0.3219 \times 10^{-4} V_i^3 - 0.01231 V_i^2 + 1.4762 V_i - 53.405$$

The corrected dynamic pressure ($\bar{q}$) in pounds per square foot was calculated from the equation

$$\bar{q} = 0.003385 V_i^2 (1. + \Delta V(2. + \Delta V/V_i^2)/V_i) \tag{8}$$

The corrected static pressure(P_s) in pounds per square foot was computed from the indicated pressure (P_i) with the relation

$$P_s = P_i - 0.003385 \Delta V(2. + \Delta V/V_i) \tag{9}$$

The expression below was determined to be a suitable representation of the engine thrust, as a function of fan percent rpm, Mach number M, ambient pressure ratio, and temperature. Defining T_r as the ratio of absolute ambient to sea level standard temperature and

$$P_r = P_s/2116.15$$
$$N_t = N/\sqrt{T_r}$$

For one engine the thrust T_n in pounds was computed as

$$T_n = P_r[(1.134 + 0.78 M^2) N_t^2 - (53.3 + 27. M^2) N_t + 6430. M^2 + 1420.]$$

11

The thrust coefficient for the four engines is calculated as

$$C_T = \sum_{n=1}^{4} \frac{T_n}{\bar{q} S} \tag{10}$$

The mass flow rate $\dot{M}$ of the air entering the engines was computed from the thrust and pressure ratio in slugs per second as follows:

$$\dot{M} = \frac{P_r}{\sqrt{T_r}} [0.4911 \times 10^{-9} (T_n/P_r)^2 + 0.00119(T_n/P_r + 2.5)] \tag{11}$$

The ram drag coefficient was calculated from the following relations, in which V_t is true airspeed in feet per second and the mass flow is summed for the four engines.

$$V_t = 29.03 \sqrt{(T_r \, \bar{q})/P_r}$$

$$C_{D_R} = \frac{V_t}{\bar{q} S} \sum_{n=1}^{4} \dot{M}_n \tag{12}$$

The side force and yawing moment data presented in this report are with the ram drag effect removed. The momentum coefficient C_μ for aileron BLC blowing (Cmu AIL in table 3) is from the relation

$$C_\mu = \frac{(V_J - V)\dot{m}_J}{\bar{q} S_{WA}} \tag{13}$$

where $\dot{m}_J$ is the mass flow rate from the BLC nozzles, V_J is the velocity of this flow, and S_{WA} is the reference area defined as the area of the wing within the region spanned by the ailerons.

In equation (1), which is the side force expression, the side acceleration is given with reference to the aircraft c.g. The accelerometer package was located in the horizontal plane of the c.g. 1.45 feet behind the quarter-chord point of the mean aerodynamic chord and 0.71 feet to the left of the plane of symmetry. The quantities X_a and Y_a in the equation below represent the distances of these instruments from the c.g. for the test conditons and are negative in sign. The acceleration was transferred to the c.g. with the equation

$$a_Y = a_{Y_i} - (X_a \dot{r} - Y_a(p^2 + r^2))/g \tag{14}$$

where a_{Y_i} is the instrument measurement.

12

REFERENCES

1. Stephenson, J. D.; and Hardy, G. H.: Longitudinal Stability and Control Characteristics of the Quiet Short-Haul Research Aircraft (QSRA). NASA TP-2065, Nov. 1989.

2. Boeing Commercial Airplane Company Staff: Quiet Short-Haul Research Aircraft Predicted Flight Characteristics. NASA CR-152203, Oct. 1979

3. Eppel, Joseph C.: Quiet Short-Haul Research Aircraft Familiarization Document, Revision 1. NASA TM-81298, Sept. 1981.

4. Stephenson, J. D.: The Application of Parameter Estimation to Flight Measurements to Obtain Lateral-Directional Stability Derivatives of an Augmented Jet-Flap STOL Airplane. NASA TP-2033, Jan. 1983.

5. Bach, R. E., Jr.: A User's Manual for AMES (A Parameter Estimation Program). NASA CR-163118, 1974.

6. Campbell, J. P.; and McKinney, M. O.: Summary of Methods for Calculating Dynamic Lateral Stability and Response and for Estimating Lateral Stability Derivatives. NASA TR-1098, 1952.

7. Cochrane, J. A.; Riddle, D. W.; Stevens, V. C.; and Shovlin, M. D.: Selected Results from the Quiet Short-Haul Research Aircraft Flight Research Program. AIAA J. Aircraft, vol. 19, no. 12, Dec. 1982.

Table 1. QSRA lateral-directional tests—initial conditions and average angles of attack

Run ID	Flt No./ run code	USB flaps, deg	DLC SPLRS, deg	Init. CL	Init. CT	Av. alpha, deg	Init. VE, kt	Init. altit., ft	Gross wt, lb
A1	361 A	48.7	0.0	5.61	0.86	15.6	70	3990	55780
A2	361 B	48.7	0.0	5.67	0.87	18.0	69	4180	55570
A3	361 C	48.7	0.0	3.04	0.38	1.1	95	7780	56000
A4	361 D	48.7	0.0	5.45	0.77	16.0	71	5800	55880
A5	430 A	48.0	0.0	5.11	1.74	2.3	70	2825	51250
A6	439 A	49.2	0.0	4.20	0.85	3.1	81	6770	56050
A7	439 B	49.2	0.0	4.30	0.88	3.1	80	5695	55950
B1	430 B	48.0	12.1	5.05	1.74	5.2	70	2435	51000
B2	452 A	49.5	13.2	4.59	1.13	6.7	78	3220	56150
C1	398 A	0.0	0.0	3.25	0.72	11.2	92	7370	55770
C2	430 D	0.0	0.0	3.42	0.79	12.3	85	2555	50360
D1	360 A	31.6	0.0	4.29	1.54	3.3	79	1750	53940
D2	360 B	31.6	0.0	5.02	1.80	9.8	72	2870	53480
E1	430 C	65.9	0.0	6.24	2.57	0.3	63	1920	50730

Table 2. QSRA lateral-directional tests—sideslip, roll rate and yaw rate derivatives

Run ID	USB flaps	CT	Alpha, deg	CLB	CNB	CYB	CLP	CNP	CYP	CLR	CNR	CYR
A1	48.7	0.86	15.6	-0.236	0.608	-2.28	-0.452	-0.395	0.048	0.962	-0.611	2.29
A2	48.7	0.87	18.0	-0.241	0.580	-2.51	-0.469	-0.449	0.208	0.944	-0.742	1.61
A3	48.7	0.38	1.1	-0.209	0.615	-2.15	-0.417	-0.108	-0.317	0.645	-0.322	1.33
A4	48.7	0.77	16.0	-0.212	0.606	-2.32	-0.439	-0.550	0.625	1.015	-0.738	2.84
A5	48.0	1.74	2.3	-0.178	0.929	-3.22	-0.458	-0.177	-0.061	0.814	-0.737	2.61
A6	49.2	0.85	3.1	-0.252	0.907	-3.33	-0.550	-0.220	-0.133	0.819	-0.580	2.53
A7	49.2	0.88	3.1	-0.283	0.920	-3.09	-0.619	-0.319	-0.225	0.855	-0.601	3.13
B1	48.0	1.74	5.2	-0.262	0.956	-3.45	-0.510	-0.148	-0.560	0.618	-0.754	2.09
B2	49.5	1.13	6.7	-0.344	0.876	-3.54	-0.583	-0.290	0.431	0.836	-0.853	3.59
C1	0.0	0.72	11.2	-0.230	0.408	-1.55	-0.483	-0.238	-0.003	0.683	-0.482	2.32
C2	0.0	0.79	12.3	-0.218	0.407	-1.49	-0.477	-0.212	-0.048	0.772	-0.525	1.79
D1	31.6	1.54	3.3	-0.272	0.779	-2.69	-0.571	-0.207	-0.475	0.724	-0.713	2.02
D2	31.6	1.80	9.8	-0.299	0.811	-2.91	-0.535	-0.456	-0.412	0.848	-0.844	2.80
E1	65.9	2.57	0.3	-0.140	0.949	-3.76	-0.617	-0.306	0.537	0.880	-0.854	3.08

Table 3. QSRA lateral-directional tests—rudder, aileron and spoiler derivatives

Run ID	USB flaps	CT	Alpha, deg	Cmu.AIL	CLRUD	CNRUD	CYRUD	CLAIL	CNAIL	CYAIL	CLSP	CNSP	CYSP
A1	48.7	0.86	15.6	0.128	(0.120)	(-0.410)	(0.600)	0.157	0.049	0.147	(0.150)	(0.014)	(0.030)
A2	48.7	0.87	18.0	0.127	(0.122)	(-0.413)	(0.600)	0.191	0.066	0.093	(0.150)	(0.014)	(0.030)
A3	48.7	0.38	1.1	0.044	0.010	-0.377	0.710	0.137	0.035	0.039	(0.150)	(0.014)	(0.060)
A4	48.7	0.77	16.0	0.113	0.097	-0.363	0.699	0.180	0.028	0.116	(0.150)	(0.014)	(0.060)
A5	48.0	1.74	2.3	0.131	0.094	-0.387	0.721	0.245	0.061	-0.142	(0.150)	(0.004)	(0.060)
A6	49.2	0.85	3.1	0.095	0.123	-0.412	0.767	0.241	0.009	0.075	(0.200)	(0.018)	(0.080)
A7	49.2	0.88	3.1	0.098	0.140	-0.447	1.416	0.178	-0.005	0.124	(0.200)	(0.018)	(0.080)
B1	48.0	1.74	5.2	0.130	0.096	-0.378	0.605	0.322	0.083	-0.139	(0.150)	(0.013)	(0.060)
B2	49.5	1.13	6.7	0.105	0.107	-0.483	1.090	0.308	0.053	-0.164	(0.150)	(0.014)	(0.030)
C1[a]	0.0	0.72	11.2	0.071	0.095	X	0.620	0.167	0.014	0.058	(0.119)	(0.017)	(0.050)
C2	0.0	0.79	12.3	0.086	0.106	-0.357	0.636	0.148	0.020	-0.026	(0.150)	(0.013)	(0.060)
D1	31.6	1.54	3.3	0.103	0.118	-0.331	0.611	0.201	0.015	0.060	(0.150)	(-0.007)	(0.040)
D2	31.6	1.80	9.8	0.123	(0.120)	(-0.363)	(0.100)	0.197	0.010	0.070	(0.150)	(0.013)	(0.060)
E1	65.9	2.57	0.3	0.113	0.166	-0.390	0.794	0.400	0.054	-0.234	(0.150)	(0.013)	(0.060)

[a]For this test, the inboard spoilers were disengaged.

Table 4. Lateral control rate derivatives

Run ID	Max splr defl, deg	CNLAT	CNSD	CLSD
A1	60.3	0.063	−0.008	−0.010
A2	60.1	0.080	−0.013	−0.010
A3	59.7	0.049	−0.007	−0.005
A4	9.6	0.042	−0.000	−0.026
A5	53.2	0.065	−0.015	−0.011
A6	20.1	0.027	−0.007	−0.016
A7	9.2	0.013	−0.005	−0.010
B1	47.6[a]	0.096	−0.007	−0.009
B2	24.7[a]	0.067	−0.004	−0.015
C1	59.6	0.031	−0.005	−0.005
C2	60.1	0.033	−0.010	−0.005
D1	34.3	0.008	−0.006	−0.016
D2	19.0	0.023	−0.011	−0.008
E1	56.2	0.067	−0.012	−0.024

[a]Measured from initial position.

16

AERODYNAMIC DATA

	WING	HORIZ	VERT
AREA (TRAP), ft²	600.0	233.0	152.0
SPAN, ft	73.5	32.0	14.0
ASPECT RATIO	9.0	4.4	1.22
TAPER RATIO	0.30	0.75	0.60
SWEEP, C4, deg	15.0	3.0	18.0
MAC in.	107.4	88.0	137.0
CHORD ROOT, in.	150.7	100.0	168.0
CHORD TIP, in.	45.2	75.0	100.0
T/C BODY SIDE, %	18.54	14	14
T/C TIP, %	15.12	12	14
INCIDENCE, deg	4.5	--	--
DIHEDRAL, deg	0.0	--	--
TAIL ARM, in.	--	525.0 in.	488.0 in.
VOL COEFF V	--	1.898	0.1402

CONTROL SURFACES

	ft²*	BLOWN
AILERON	32.2	BLC
FLAPS INBD	105.0	USB
FLAPS OUTBD	40.2	NONE
SPOILERS	33.7	NONE
L.E. FLAPS	54.3	NONE
ELEVATOR	81.6	NONE
RUDDER	60.8	NONE

*THEORETICAL RETRACTED AREA

DIMENSIONS IN m(ft)

Figure 1. QSRA general arrangement.
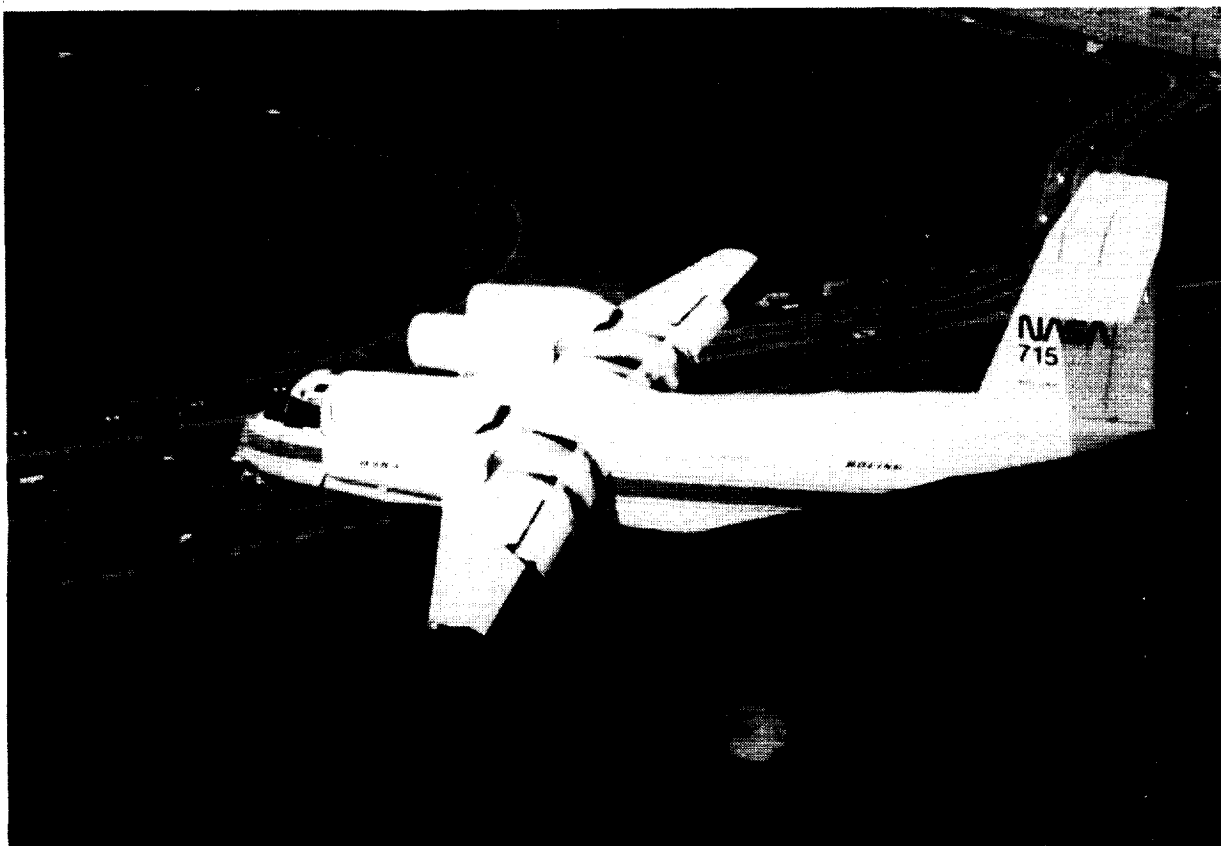
Figure 2. Photograph of the QSRA in a landing-approach configuration.
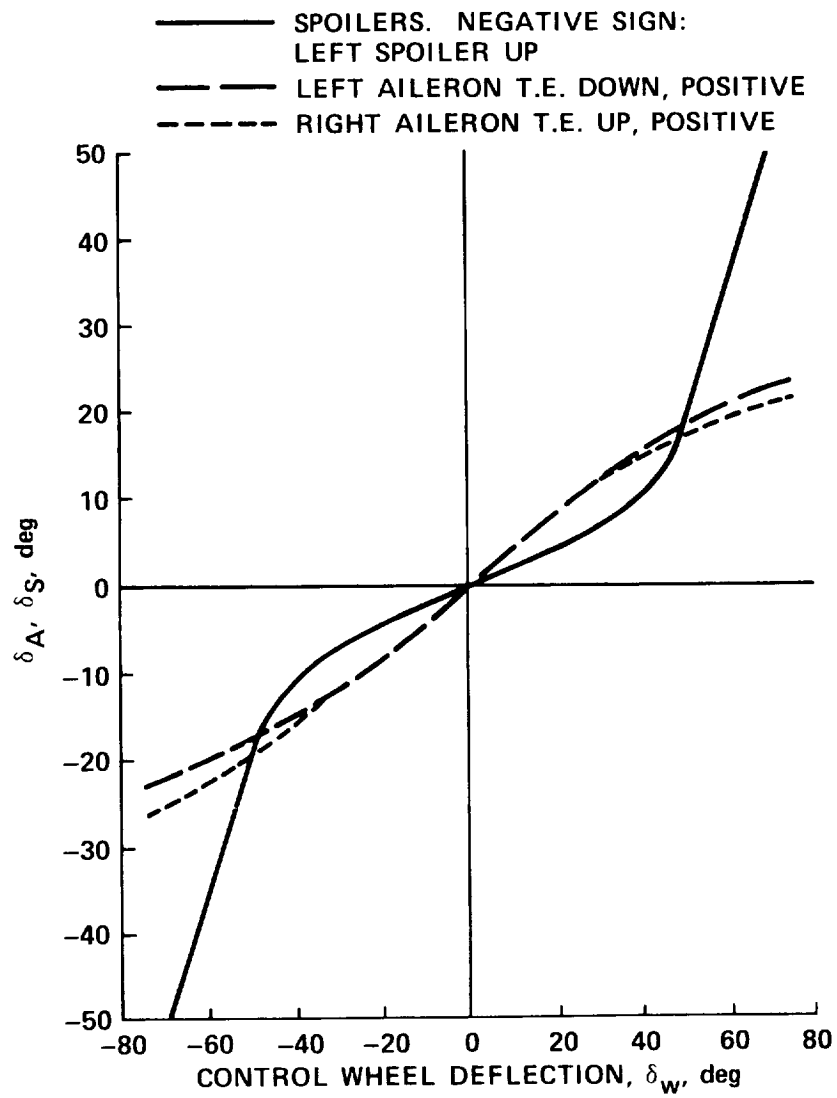
Figure 3. Static calibration of the aileron deflection and the spoiler deflection as functions of the control-wheel angle.
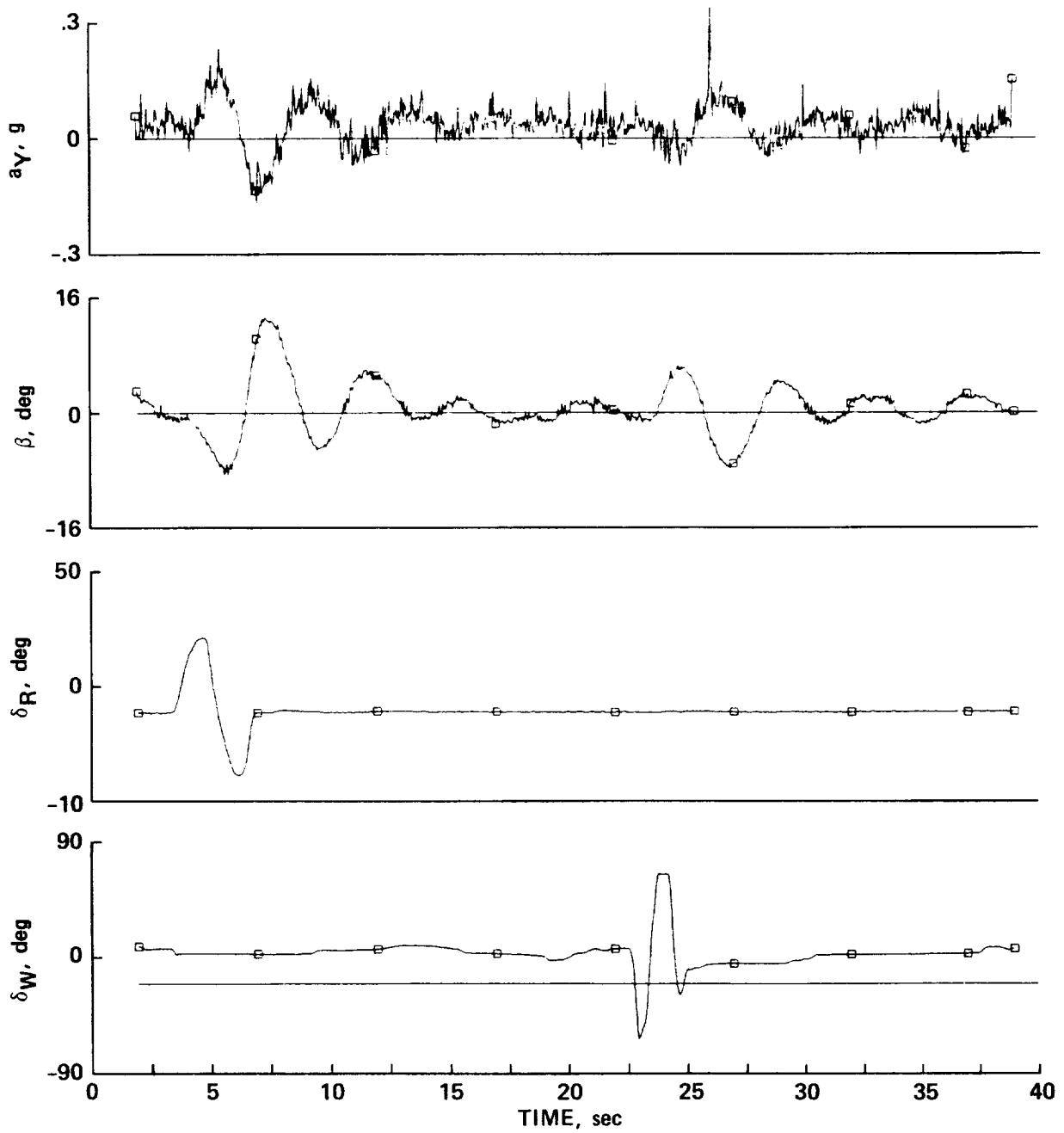
Figure 4. Time-history record of a typical maneuver resulting from a rudder input followed by a control-wheel input. Test A5. (a) a_Y, β, δ_R, and δ_W.

(b)

Figure 4. Concluded. (b) α, ϕ, r, and p.

240,000

I_x SLUG-ft^2

200,000

160,000

440,000

I_z SLUG-ft^2

420,000

400,000

380,000

26,000

I_{xz} SLUG-ft^2

22,000

18,000

40   44   48   52   56   60 x 1000
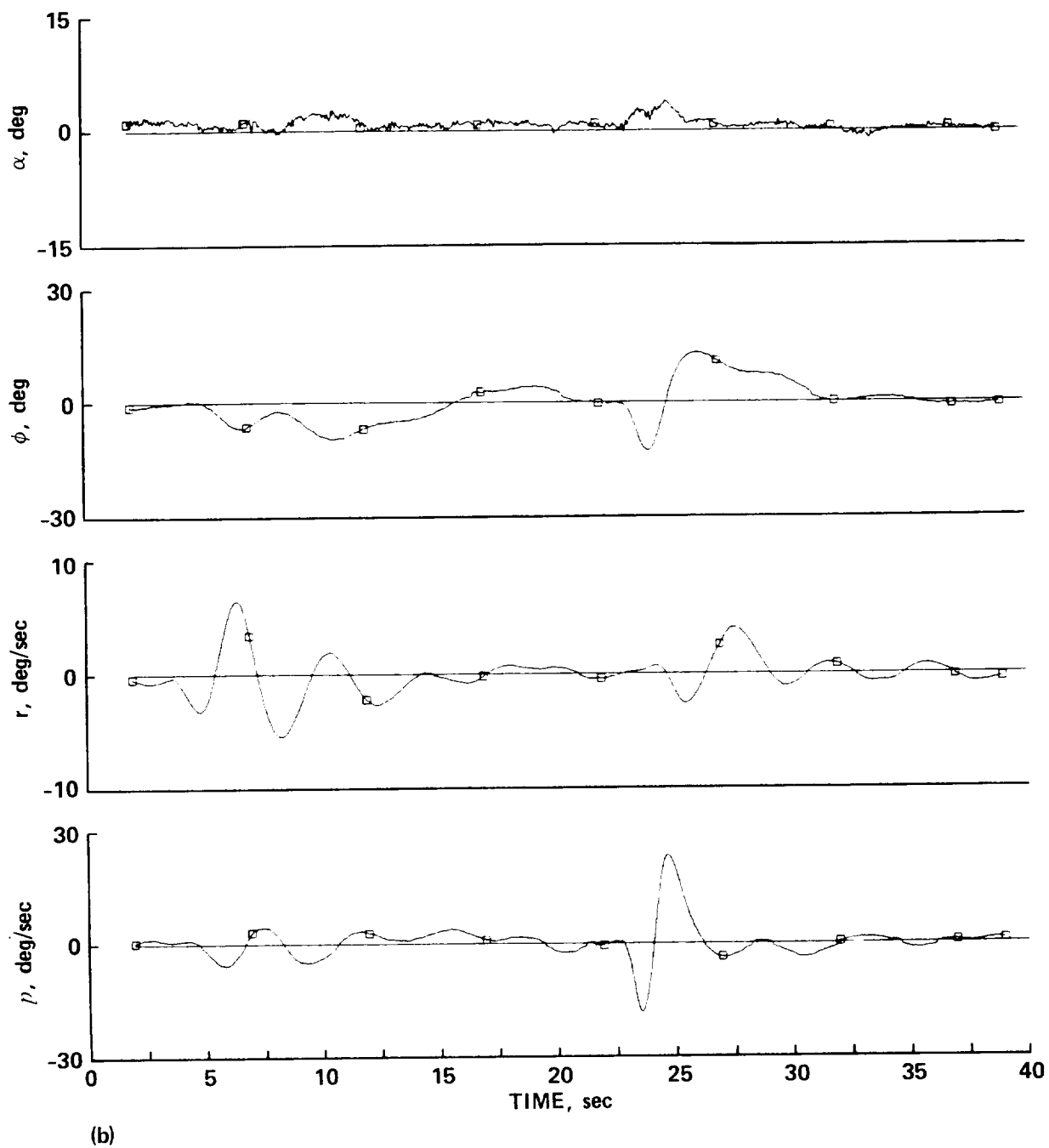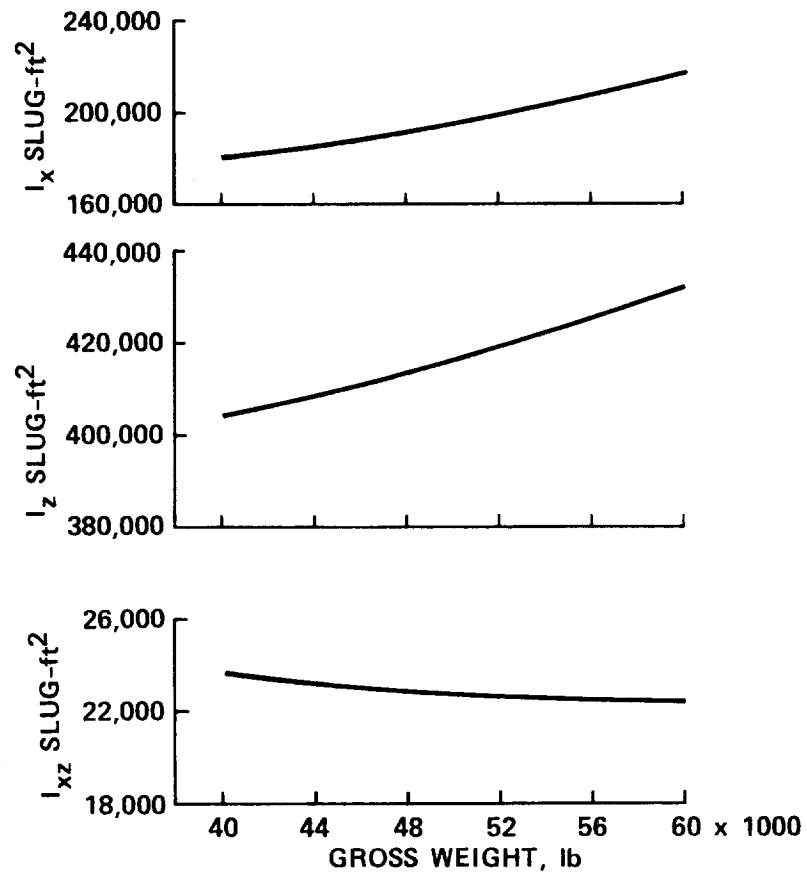
GROSS WEIGHT, lb

Figure 5. QSRA moments of inertia, I_x and I_z, and product of inertia, I_{xz}, as functions of gross weight.
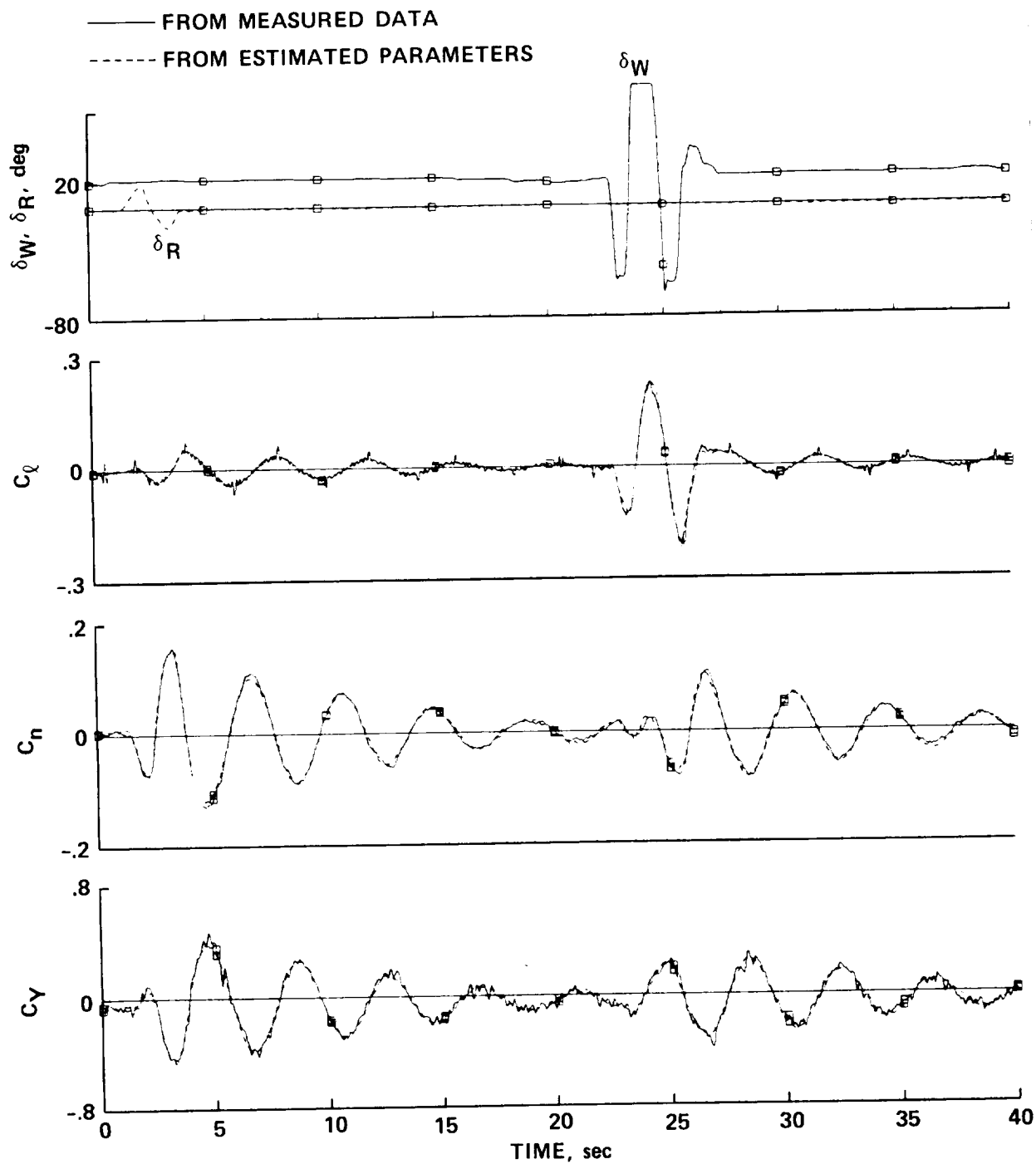
Figure 6. Comparison of the time histories of C_l, C_n, and C_Y computed with measured and with estimated parameters. USB flaps, 50°, Test A3.
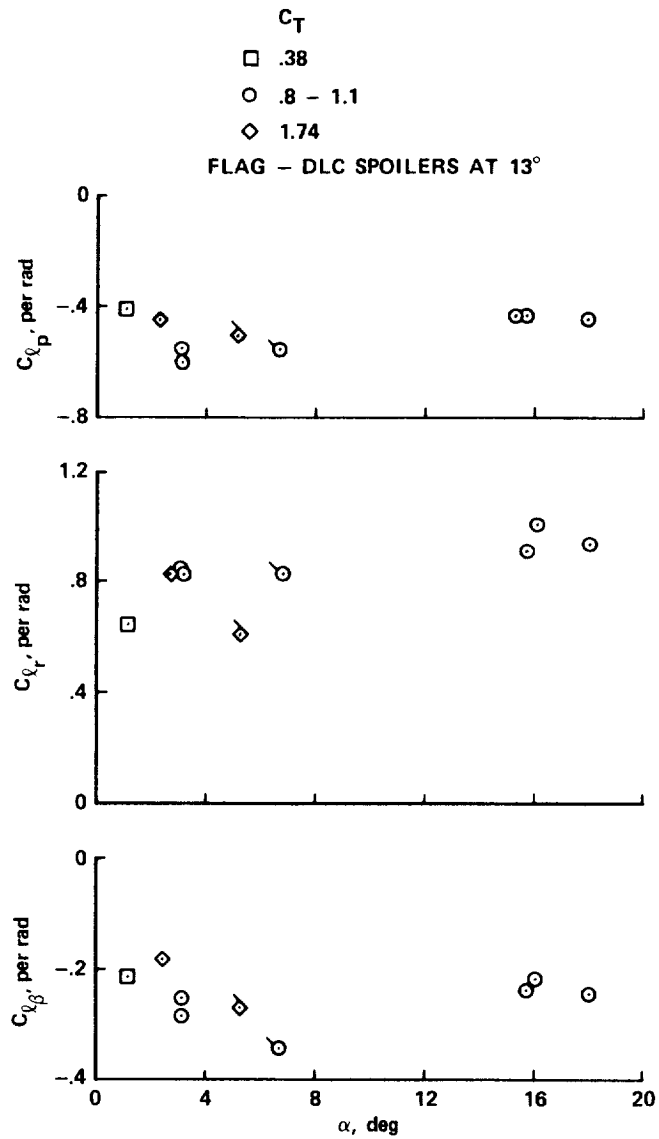
Figure 7. Lateral-directional stability derivatives for the QSRA with the USB flaps deflected 50°. (a) Rolling-moment derivatives.
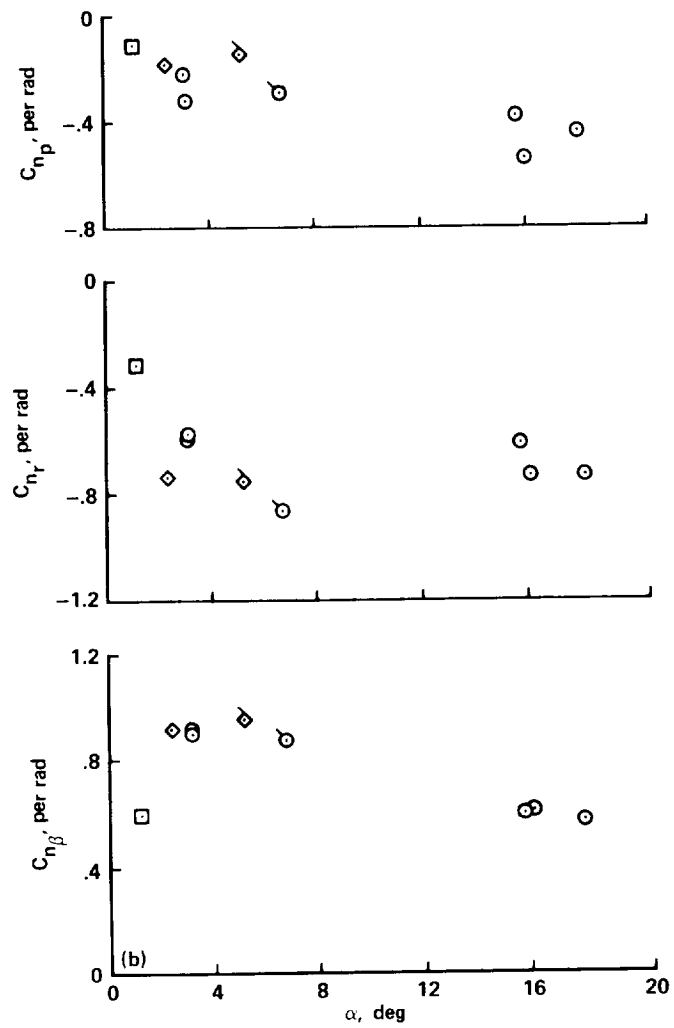
Figure 7. Continued. (b) Yawing-moment derivatives.
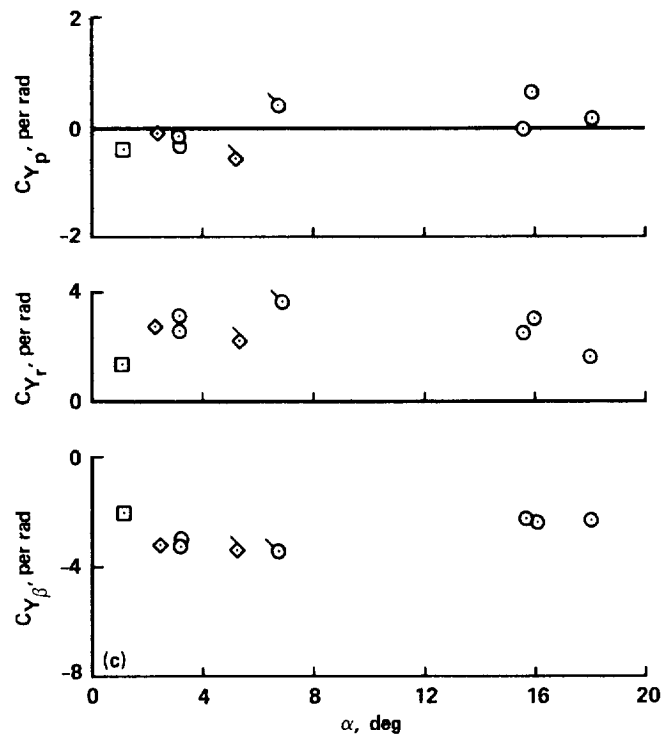
Figure 7. Concluded. (c) Side-force derivatives.
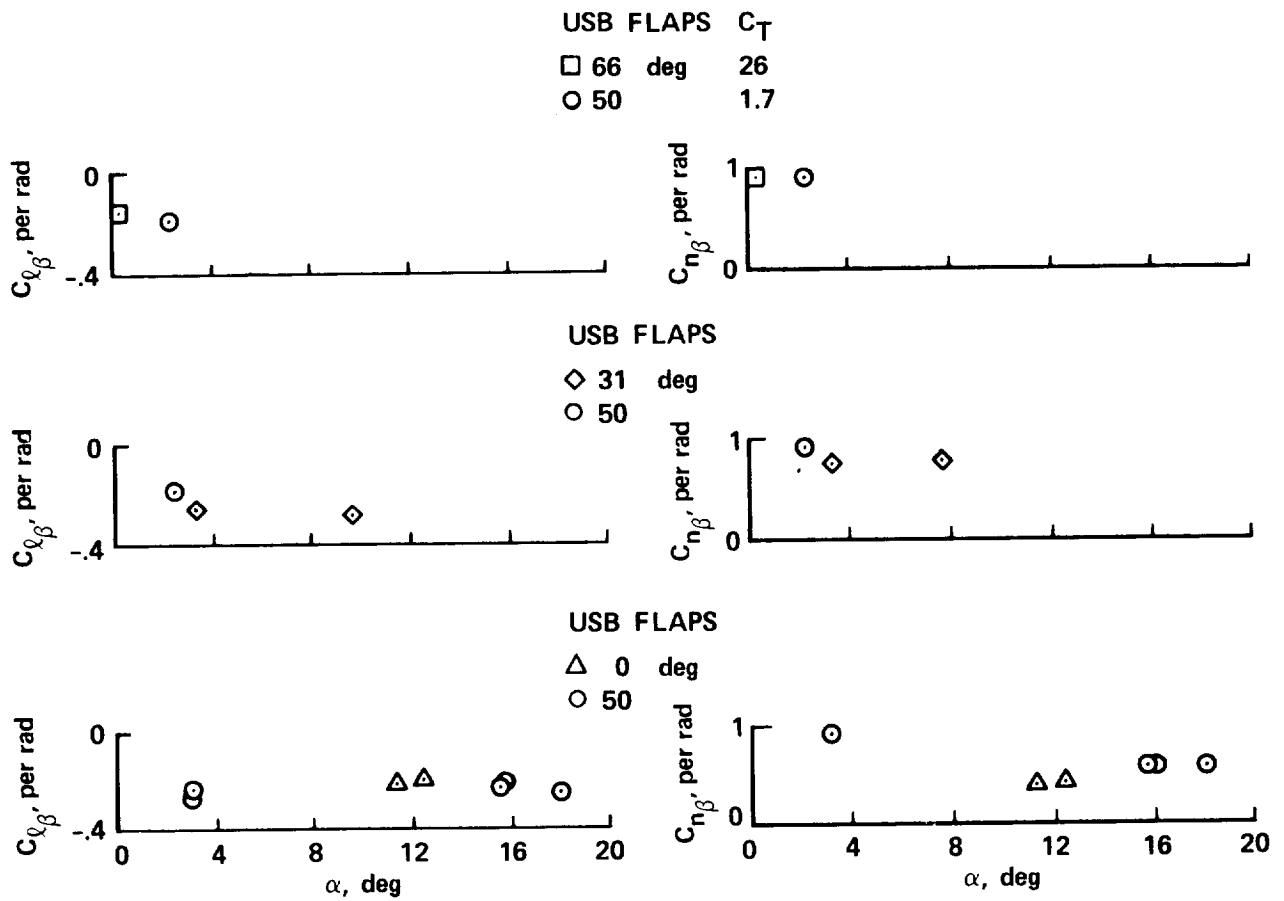
Figure 8. Sideslip derivatives, C_{l_β} and C_{n_β}, vs α, for the QSRA with the USB flaps deflected 0°, 31°, and 66°, compared with the derivatives for 50° flap deflection.
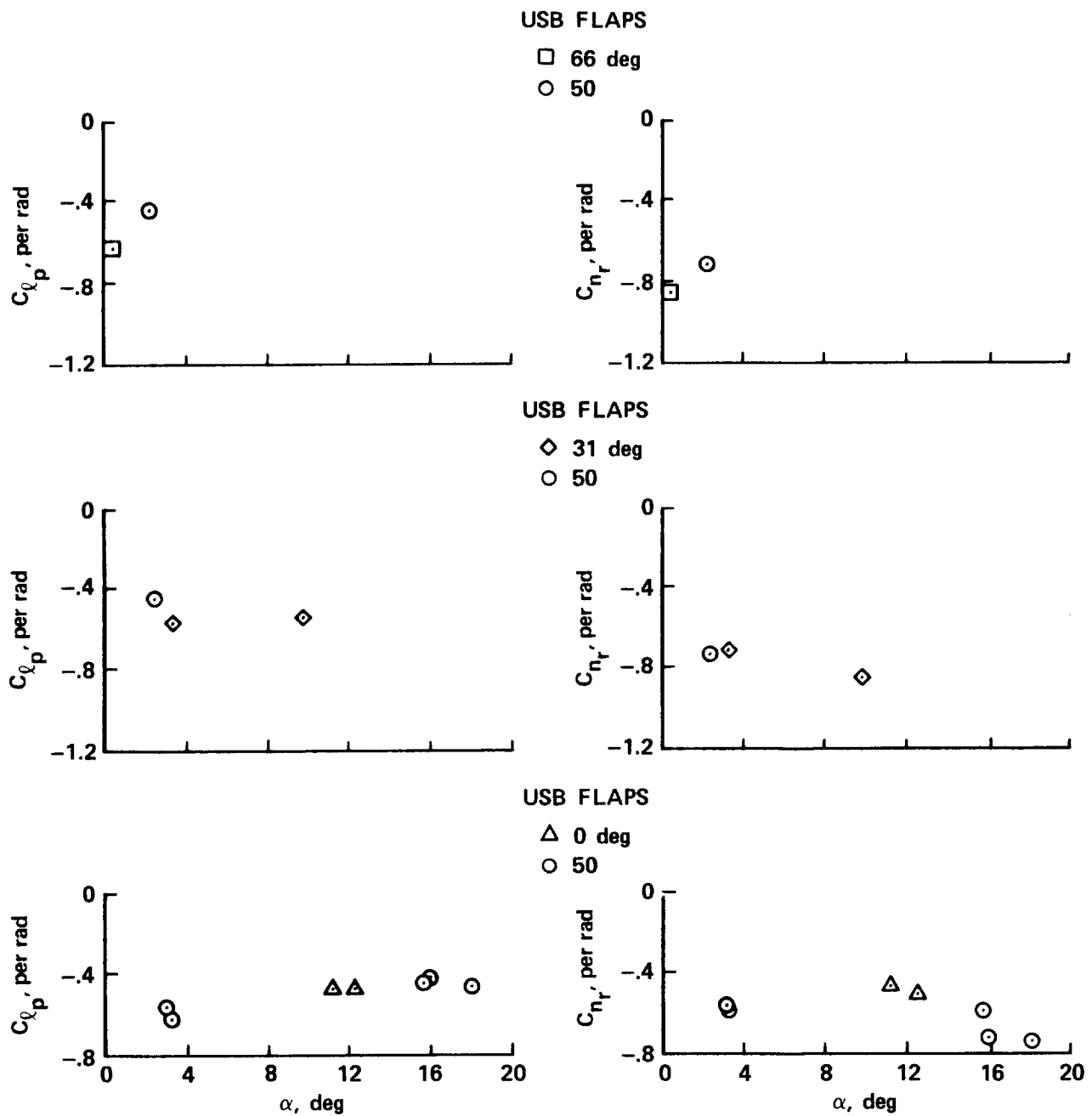
Figure 9. Roll- and yaw-damping derivatives vs α for the QSRA with the USB flaps deflected 0°, 31°, and 66°, compared with damping estimates for the aircraft with the flaps at 50°.
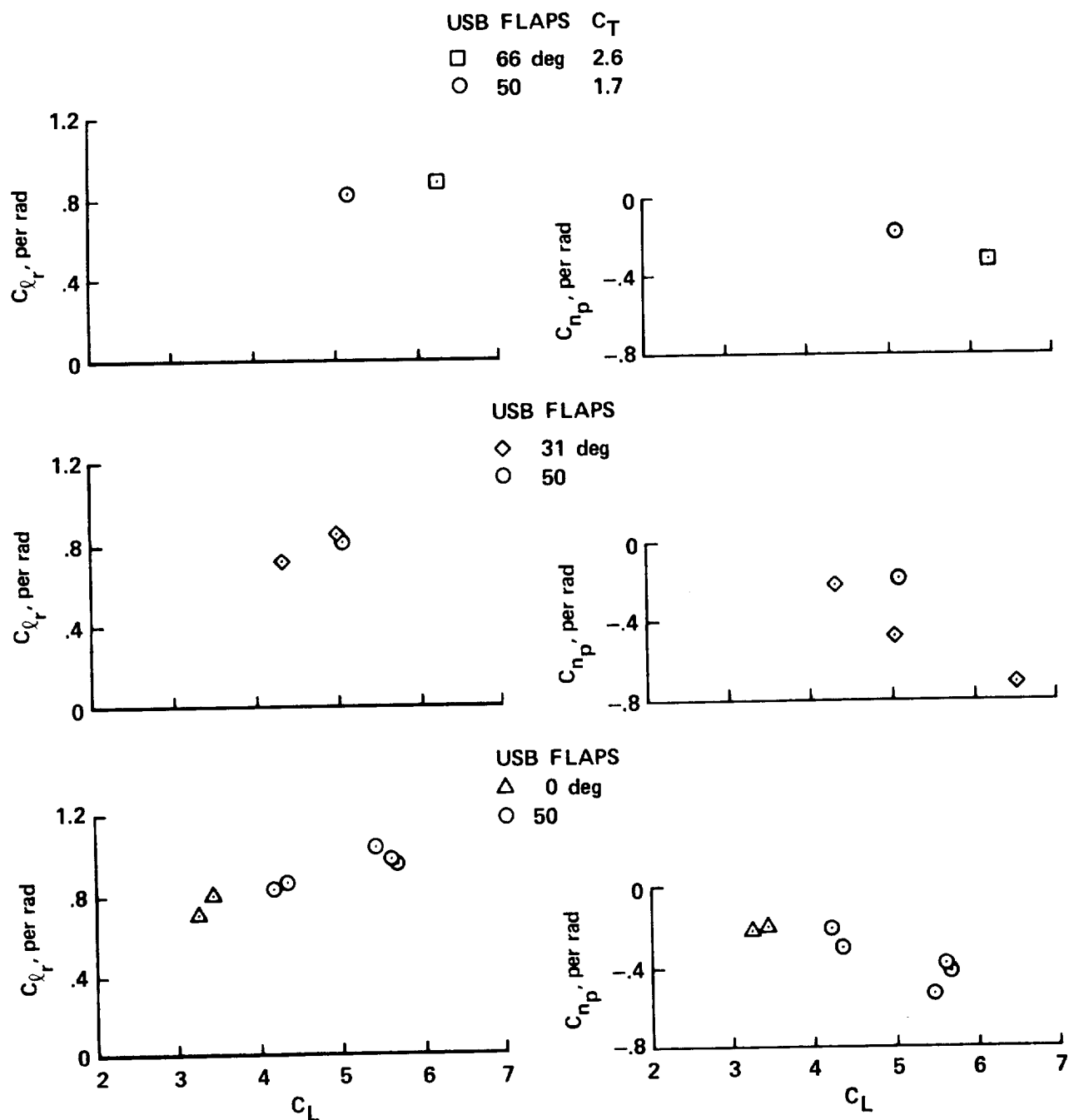
Figure 10. Cross derivatives, C_{l_r} and C_{n_p}, as functions of lift coefficient. USB flaps, 0°, 31°, and 66°, compared with the derivatives for 50° flap deflection.
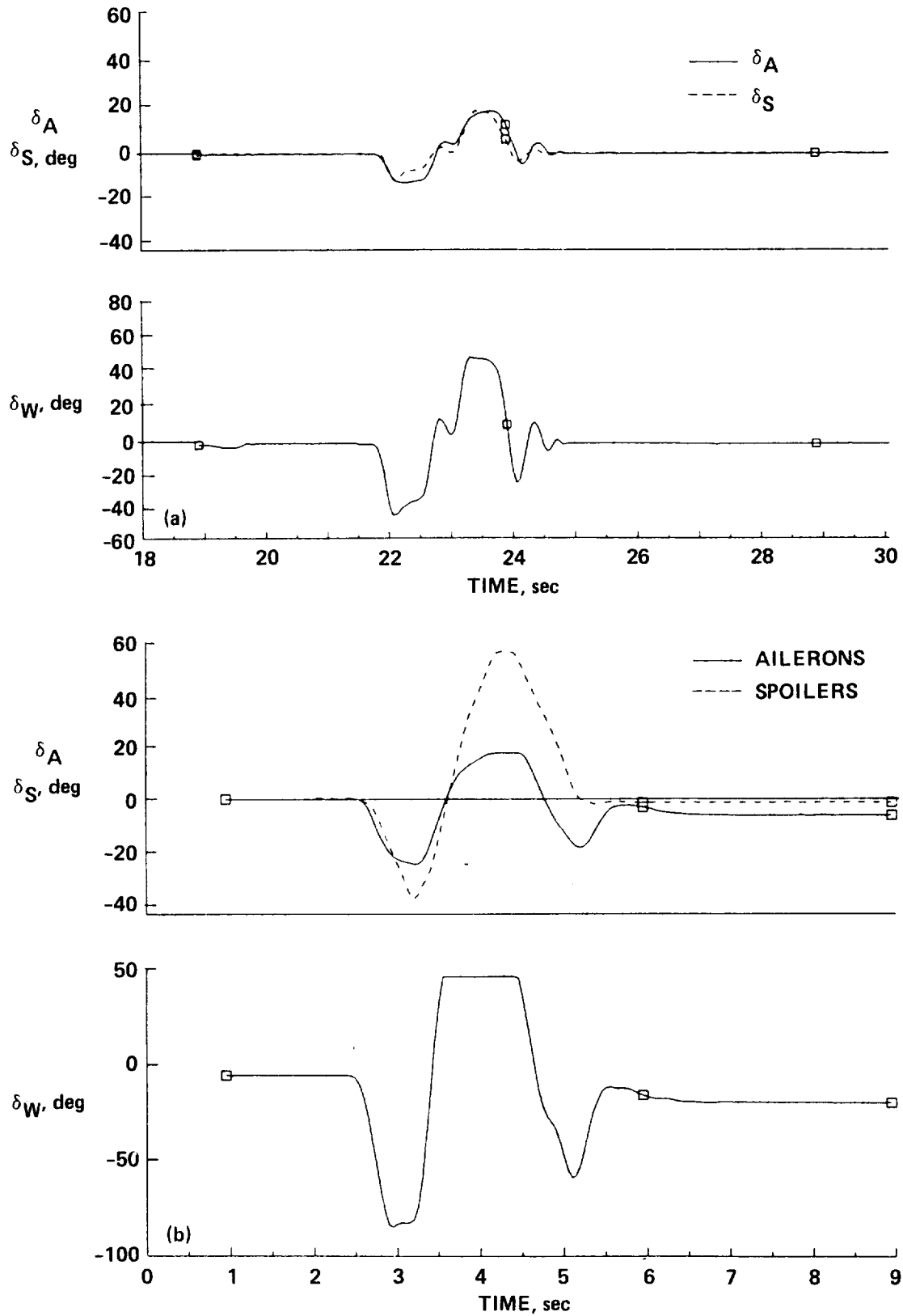
Figure 11. Time-history records of the aileron and spoiler deflections from two maneuvers having different control-wheel input variations. (a) Input with small maximum wheel angle. Test A6. (b) Input with large maximum wheel angle. Test A1.
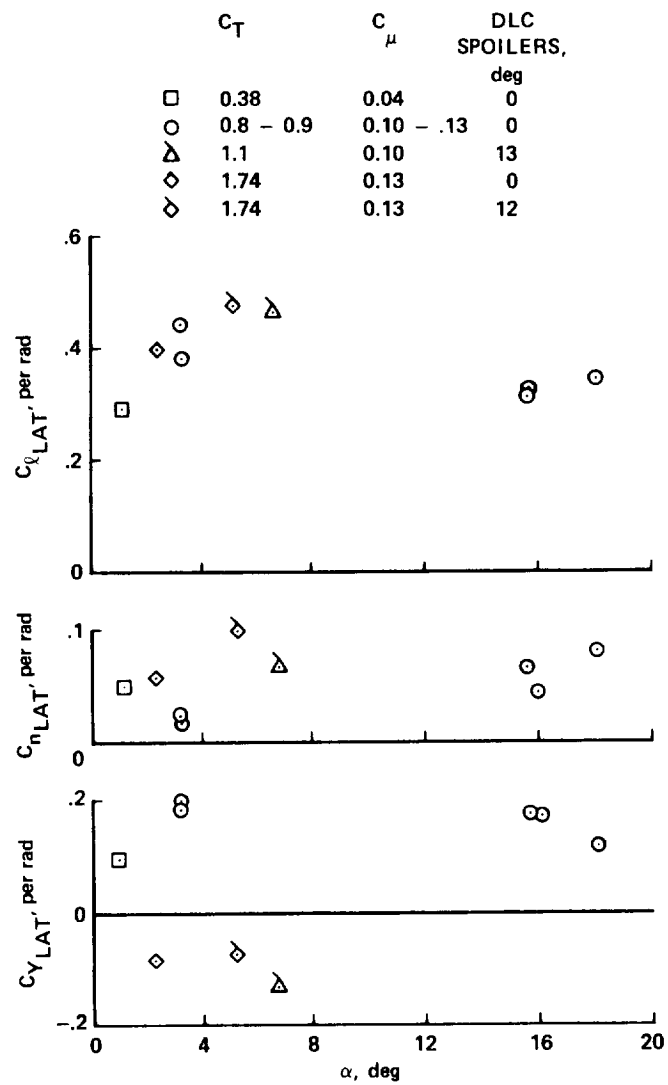
Figure 12. Variation of the rolling-moment, yawing-moment, and side-force coefficients with lateral control deflection vs α; USB flaps at 50°.
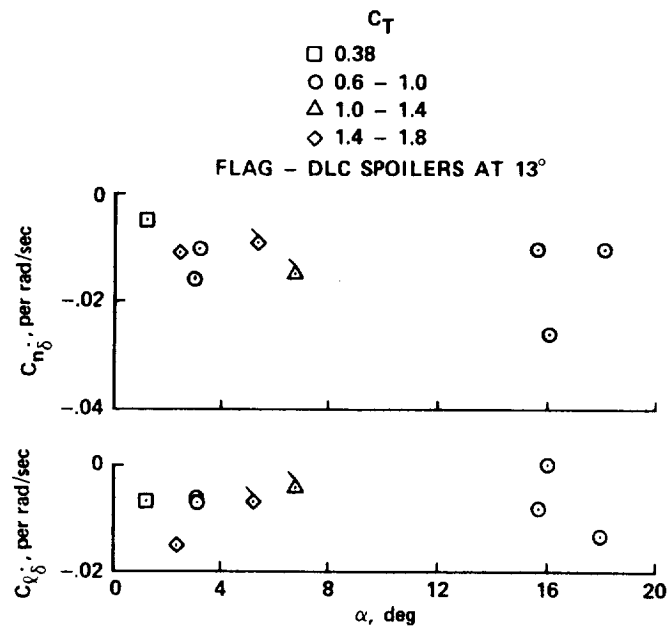
Figure 13. Variation of the rolling- and yawing-moment coefficients with rate of deflection of the spoilers. USB flaps, 50°.

1. Report No. NASA TM-102250	2. Government Accession No.	3. Recipient's Catalog No.
4. Title and Subtitle Lateral-Directional Stability and Control Characteristics of the Quiet Short-Haul Research Aircraft (QSRA)		5. Report Date May 1990
		6. Performing Organization Code
7. Author(s) Jack D. Stephenson, James A. Jeske, and Gordon H. Hardy		8. Performing Organization Report No. A-90007
		10. Work Unit No. 505-61-71
9. Performing Organization Name and Address Ames Research Center Moffett Field, CA 94035-1000		11. Contract or Grant No.
12. Sponsoring Agency Name and Address National Aeronautics and Space Administration Washington, DC 20546-0001		13. Type of Report and Period Covered Technical Memorandum
		14. Sponsoring Agency Code

15. Supplementary Notes

Point of Contact: Jack D. Stephenson, Ames Research Center, MS 211-2
Moffett Field, CA 94035-1000
(415) 604-6004 or FTS 464-6004

16. Abstract

This report presents the results of flight experiments to determine the lateral-directional stability and control characteristics of the Quiet Short-Haul Research Aircraft (QSRA), an experimental aircraft designed to furnish information on various aerodynamic characteristics of a transport type of airplane that makes use of the upper-surface blown (USB) flap technology to achieve short takeoff and landing (STOL) performance. The flight program designed to acquire the data consisted of maneuvers produced by rudder and control-wheel inputs with the airplane in several configurations that had been proposed for landing approach and takeoff operation. The normal stability augmentation system was not engaged during these maneuvers. Time-history records from the maneuvers were analyzed with a parameter estimation procedure to extract lateral-directional stability and control derivatives. For one aircraft configuration in which the USB flaps were deflected 50°, several maneuvers were performed to determine the effects of varying the average angle of attack, varying the thrust coefficient, and setting the airplane's upper surface spoilers at a 13° symmetrical bias angle. The effects on the lateral characteristics of deflecting the spoilers were rather small and generally favorable. The data indicate that for one test, conducted at low thrust (a thrust coefficient of 0.38), compared with results from tests at thrust coefficients of 0.77 and larger, there was a significant decrease in the lateral control effectiveness, in the yaw damping and in the directional derivative (C_{n_β}). The directional derivative was also decreased (by about 30%) when the average angle of attack of the test was increased from 3° to 16°.

17. Key Words (Suggested by Author(s)) STOL aircraft, Lateral-directional stability, Powered lift aircraft, QSRA flight research	18. Distribution Statement Unclassified-Unlimited Subject Category - 08		
19. Security Classif. (of this report) Unclassified	20. Security Classif. (of this page) Unclassified	21. No. of Pages 33	22. Price A03